Journal of The Electrochemical Society, **164** (9) A1802-A1811 (2017)
0013-4651/2017/164(9)/A1802/10/$37.00 © The Electrochemical Society

Sensitivity and Limitations of Structures from X-ray and Neutron-Based Diffraction Analyses of Transition Metal Oxide Lithium-Battery Electrodes

Hao Liu,[a] Haodong Liu,[b] Saul H. Lapidus,[a] Y. Shirley Meng,[b,*] Peter J. Chupas,[c,z] and Karena W. Chapman[a,z]

[a]*X-ray Science Division, Advanced Photon Source, Argonne National Laboratory, Argonne, Illinois 60439, USA*
[b]*Department of NanoEngineering, University of California-San Diego, La Jolla, California 92093-0448, USA*
[c]*Photon Sciences Directorate, Advanced Photon Source, Argonne National Laboratory, Argonne, Illinois 60439, USA*

Lithium transition metal oxides are an important class of electrode materials for lithium-ion batteries. Binary or ternary (transition) metal doping brings about new opportunities to improve the electrode's performance and often leads to more complex stoichiometries and atomic structures than the archetypal $LiCoO_2$. Rietveld structural analyses of X-ray and neutron diffraction data is a widely-used approach for structural characterization of crystalline materials. However, different structural models and refinement approaches can lead to differing results, and some parameters can be difficult to quantify due to the inherent limitations of the data. Here, through the example of $LiNi_{0.8}Co_{0.15}Al_{0.05}O_2$ (NCA), we demonstrated the sensitivity of various structural parameters in Rietveld structural analysis to different refinement approaches and structural models, and proposed an approach to reduce refinement uncertainties due to the inexact X-ray scattering factors of the constituent atoms within the lattice. This refinement approach was implemented for electrochemically-cycled NCA samples and yielded accurate structural parameters using only X-ray diffraction data. The present work provides the best practices for performing structural refinement of lithium transition metal oxides.
 [DOI: 10.1149/2.0271709jes]

Manuscript submitted March 16, 2017; revised manuscript received May 15, 2017. Published June 21, 2017.

Most electrodes used in Li-ion batteries are based on first-row transition metal oxides, such as layered structures related to $LiCoO_2$[1] and spinel-type $LiMn_2O_4$.[2] Energy storage in these materials is realized via an intercalation mechanism; Li ions are reversibly inserted into and extracted from the redox-active transition metal oxide lattice. Strategies to optimize the electrochemical performance of these systems, through substitution of the transition metal ion ($LiNi_xMn_yCo_{1-x-y}O_2$)[3] and intergrowth of different structure types, such as $xLi_2MnO_3 \cdot (1\text{-}x)LiMO_2$ (M = Ni, Co, Mn, etc),[4] have yielded next generation electrodes of increasing structural and compositional complexity. Understanding the structure and distribution of redox-active species and Li within these transition metal oxide electrodes,[5,6] and how these evolve during electrochemical cycling or over extended cycling, is critical to guiding the development of next generation electrodes and mitigating the processes that lead to decreased electrochemical performance (capacity loss, voltage fade, etc).

Crystallographic analysis of diffraction data is widely used to probe the atomic structure of electrode materials; the positions of atoms within a crystalline electrode phase can be located with high precision. However, for electrode materials with increasingly complex mixed-metal stoichiometry and cation site disorder (also referred to as "site mixing"), we are pushing the diffraction data to evaluate a growing number of structural parameters. If the additional structural parameters introduced by mixed metal stoichiometry are not adequately constrained by the data, refinement of these parameters may be correlated, preventing simultaneous determination of all structural parameters and contributing to systematic errors in the refined values. The diffraction data must be modeled with increasing care and consideration of the characteristics of the diffraction probes to reliably distinguish and quantify the distribution of different elements and species.

As the diffraction, typically of X-rays or neutrons, data are derived from elastic scattering processes, the ability to distinguish atoms of different elements depends on the difference in their respective scattering power. The different scattering physics of X-ray and neutron also compound the determination of the best structural model that is consistent with both neutron and X-ray diffraction data.

- Scattering of X-rays by an atom, in an X-ray diffraction (XRD) measurement, involves interactions with the electrons; the X-ray scattering factor (Figure 1a) is proportional to the number of electrons in the atom and, due to spatial delocalization of the electron density, the X-ray scattering factor reduces with increasing scattering vector, Q ($Q = 4\pi \sin\theta/\lambda$, θ, and λ are the diffraction angle and the wavelength, respectively). With X-ray scattering being proportional to the number of electrons, elements close in atomic number (i.e., all first-row transition metals) are poorly distinguished. The contribution from light elements (e.g. Li, O) can be challenging to distinguish in the presence of heavier elements. As different oxidation states of a given element have a different number of electrons, the scattering

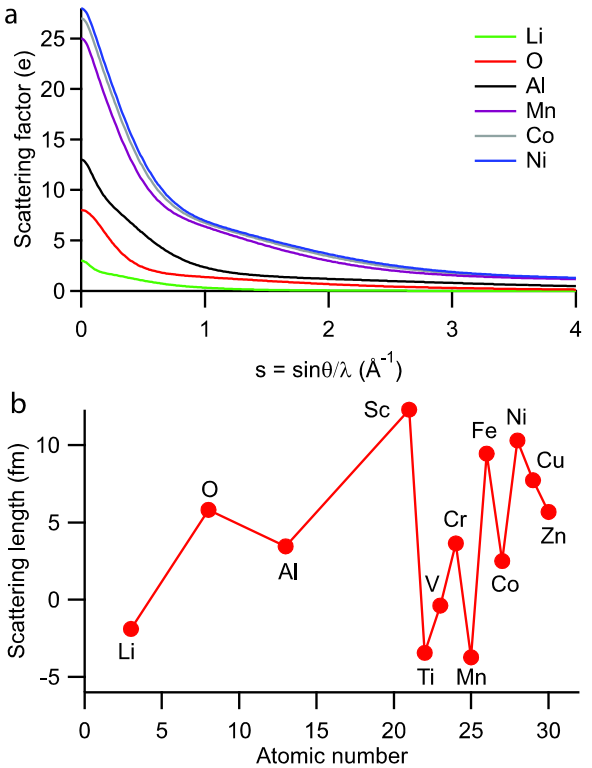

Figure 1. (a) The X-ray scattering factor[30] of select atoms and (b) the coherent neutron scattering length[31] of Li, O, Al and the first-row transition metals.

*Electrochemical Society Member.
[z]E-mail: chupas@aps.anl.gov; chapmank@aps.anl.gov

contribution from the redox-active transition metal within the electrode will vary depending on the state of charge.

- Scattering of neutrons (Figure 1b), in a neutron diffraction (ND) measurement, involves interaction with the atomic nuclei; the neutron scattering length (1) varies irregularly with atomic number and isotope and is (2) not Q-dependent. The variability of neutron scattering length (e.g. with very different scattering lengths for Ni and Co) can be used to help distinguish species of low and similar atomic number. The Q-independence of the scattering length makes ND a better approach than XRD to determine the atomic displacement parameters.

A number of studies[7,8] analyzed both XRD and NPD data, but direct co-refinement of X-ray and neutron diffraction data for battery systems is relatively rare.[9] However, co-refinement of XRD and NPD data has been successfully applied to understand other systems containing light elements, such as hydrogen,[10] and complex structures with a large number of atoms and positional parameters.[11]

Here we explore the sensitivity and limitations of X-ray and neutron powder diffraction in resolving mixed-metal stoichiometry and structural defects in complex substituted transition metal oxide electrodes, focusing on $LiNi_{0.8}Co_{0.15}Al_{0.05}O_2$ (NCA)[12] as an exemplar. In such electrode materials, doping the transition metal site with a few percent of a different species can have a dramatic impact on the electrochemical performance.[13] Similarly, increasing the Li-Ni cation mixing has been linked to a large reduction in energy storage capacity (by a factor of 2).[14] By comparing different refinement strategies involving analysis of X-ray data only, neutron data only or combined X-ray-neutron data, analysis using X-ray scattering factors for different oxidation states, and analysis over different Q-ranges, we evaluate the precision/accuracy with which the Ni, Co and Al stoichiometry, the occupancies of Li and O, and the extent of the cation mixing, can be determined. The optimized refinement strategy was then applied to samples of NCA recovered following electrochemical cycling to evaluate the associated changes in their structure and ion distribution.

Experimental

Structural model.—The structural model for NCA is described in the R-3m space group with the Ni, Co and Al on the 3a site, Li on the 3b site, and O on the 6c site (Figure 2a). Cation mixing between Li and Ni, which is routinely observed due to their similar cation size,[6] is modeled by allowing Ni and Li occupancy (in equal quantity) on the 3b (Li) and 3a (transition metal) sites, respectively. Accordingly, the relationship between site occupancy factors for different atoms can be described by the following equation:

$$n_{3a}^{Li} = n_{3b}^{Ni} = 1 - n_{3a}^{Ni} - n_{3a}^{Co} - n_{3a}^{Al} \quad [1]$$

where n_i^M corresponds to the occupancy of the atom M on the Wyckoff site i. The total occupancy of atoms on the 3a site is constrained to be 1 in the model; if there is incomplete occupancy (i.e. vacancies) at the 3a site (transition metal layer), this will lead to refined occupancies greater than 1 on the 3b (Li layer) and/or 6c (O layer) site. Atomic displacement parameters (ADPs) for atoms occupying the same Wyckoff positions are constrained to be the same. Since the lattice parameters are only reflected in the Bragg peak positions and not the intensities, the lattice parameters can be determined independently of a structural model and are not discussed here.

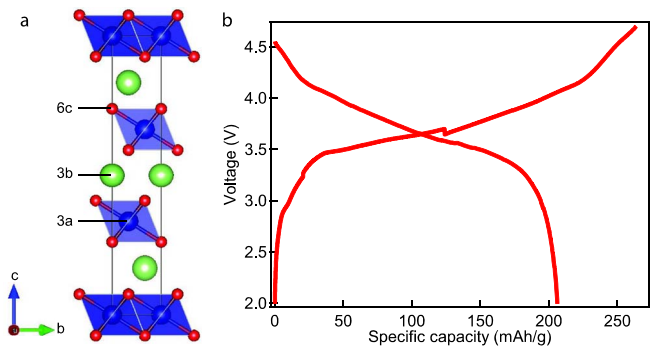

Figure 2. (a) Crystal structure of NCA. The blue (Ni, Co and Al), green and red spheres correspond to the transition metals and Al, Li, and O, respectively. (b) Typical charge and discharge profiles of the NCA/meso carbon micro bead full cell.

Neutron and X-ray powder diffraction measurement.—For the pristine NCA sample, time of flight (TOF) powder neutron diffraction data was collected on the POWGEN instrument at the Spallation Neutron Source (SNS) in the Oak Ridge National Lab (ORNL). Around 3 g of powder was filled into a vanadium sample can and sent via the mail-in service to the SNS. Data were collected at a wavelength of 1.066 Å to cover a d-spacing range of 0.3−3.0 Å.

For charged/discharged NCA samples, TOF data were collected at the VULCAN instrument at the Spallation Neutron Source (SNS), Oak Ridge National Laboratory. At VULCAN, approximately 1.6 g of powder was loaded into a vanadium sample can of 6 mm diameter. An incident beam (5 mm × 12 mm) of 0.7 to 3.5 Å bandwidth, allowing 0.5∼2.5 Å d-space in the diffracted pattern of the ±90° 2θ detector banks, was selected using the double-disk choppers at 30 Hz frequency. The high-resolution mode was employed with Δd/d ∼0.25%. The SNS was at nominal, 1100 kW, power. Powder neutron diffraction data were collected in the high-resolution mode for a duration of 3 h and processed using VDRIVE software.[15] The data was normalized to a vanadium rod.

High-resolution XRD measurement was performed at beamline 11-BM with multiple single-crystal analyzer detectors, at the Advanced Photon Source, Argonne National Laboratory. Samples were loaded into 0.80 mm inner diameter polyimide tubes in an argon-atmosphere glove box. Powder diffraction patterns were measured in 0.001° steps (2θ) with 0.1 s per step between 0.5° and 40° for the pristine sample and between 0.5° and 36° for the electrochemically-cycled samples. The pristine and the electrochemically-cycled NCA samples were measured at 0.459990 and 0.414215 Å, respectively.

Rietveld structural refinement.—Rietveld refinement was performed with TOPAS software package.[16] The background was described by a 9-term Chebyshev polynomial. For refinement against NPD patterns, the TOF profile function 3, as implemented in GSAS,[17] was used. For refinement against XRD patterns, the peak profile was described by isotropic broadening due to domain size and anisotropic broadening due to strain.[18]

Sample preparation.—$LiNi_{0.8}Co_{0.15}Al_{0.05}O_2$ was purchased from TODA America (NAT1050). The nominal chemical composition is used to denote the sample.

Electrochemical cycling of NCA was performed in pouch cells designed and assembled in a dry room at NIMTE's (Ningbo Institute of Materials Technology & Engineering) fabrication facility. The cell includes 10 pieces of dual sided meso carbon micro bead (MCMB) anode and NCA cathode. The cathode is composed of 92 wt% NCA, 5 wt% super P and 3 wt% polyvinylidene fluoride on an aluminum current collector. The anode is composed of 91 wt% MCMB, 4 wt% super P, 2 wt% carboxymethyl celluloseand, 3 wt% styrene-butadiene rubber on a copper current collector. A Celgard separator is used to alternatively cover the anode and cathode on each side. The electrolyte solution composed of 1 M $LiPF_6$ in a 3:7 (volume ratio) ethylene carbonate: dimethyl carbonate (DMC). Typical charge and discharge profiles are shown in Figure 2b. The cycled electrodes were recovered by disassembling cycled pouch cells in an argon-atmosphere glove box. The cathode was washed with DMC three times and dried in Ar-atmosphere overnight. The NCA powders were scraped off the Al current collector for structural analysis.

Results and Discussion

Selecting structural parameters for Rietveld refinement.—The number and type of structural parameters that can be reliably refined are dictated by the type (neutron or X-ray diffraction) and quality of the powder diffraction data. Refining more parameters than are adequately constrained by the diffraction data will lead to a high correlation (>70%) between the parameters. A high correlation between two parameters indicates that changes in either of the parameters would yield the same (for 100% correlation) or similar (for high correlation) effects on the refinement. Attempts to refine all site occupancy factors, including the mixed metal stoichiometry and the Li-Ni mixing, against only the neutron or X-ray diffraction data resulted in high correlations of these parameters (Table S1). This indicates that neither the NPD nor XRD data alone provides sufficient information to evaluate the stoichiometry of NCA. We found that refining only the anisotropic ADPs of atoms on the 3a and 3b sites, the Li occupancy on 3b site, the O occupancy on 6c site, and the z coordinate of O eliminates these correlations (Table S2), while constraining the isotropic ADP of Li on 3b site and Co, Al and Li-Ni site mixing occupancies to constant values.

Diffraction aberrations due to absorption occur in both NPD and XRD measurements. For NPD, ^{6}Li (7.5% natural abundance) has a large absorption cross section, but refinement of the absorption coefficient yields a small value (<0.1), suggesting a minor effect of absorption on the result here. The use of ^{7}Li-enriched sample can in principle mitigate the absorption effect, yet a previous NPD study of $^7LiCoO_2$ found that enrichment with ^{7}Li was not as effective as measuring over a larger Q-range for obtaining accurate structural parameters.[19] Additionally, the absorption correction is applied as a product of a scale factor and an ADP factor, which will underestimate the ADPs[20] but will have little effect on positional and occupational parameters. For XRD, the absorption factor is highly correlated with the ADPs, and excluding this factor from refinement leads to underestimated ADPs but has little effects on other structural parameters. Therefore, the absorption factor is not included in the NDP and XRD refinements at the expense of a systematic underestimation of the ADPs.

Since some structural parameters have to be constrained, the refinement will yield different values depending on the values assigned for the constrained structural parameters. This could lead to erroneous results when the constrained parameters are not well characterized by other methods. For example, the nominal stoichiometry may deviate from the actual stoichiometry, and compositional heterogeneity may lead to a distribution of stoichiometry for individual crystallites. Consequently, the variation in the refined structural parameters introduced by uncertainty in the constrained structural parameter could be higher than the estimated standard deviation (esd) from the refinement. In the following sections, we evaluate the impact of variations in the constrained structural parameters on the refined structural parameters in NCA.

Rietveld refinements against only NPD data for pristine NCA.—We performed Rietveld refinement against only the NPD pattern (Figure 3) with the nominal Ni, Co and Al stoichiometry ($Ni_{0.8}Co_{0.15}Al_{0.05}$) and no Li-Ni mixing, which yields errors (esd) of <0.01 for Li and O occupancies, 0.00004 for O coordinate, and 0.03 Å^2 for the anisotropic ADPs of Ni, Co, Al and O (Table S3). To evaluate the impact of uncertainty in constrained parameters on the refinement results, we performed a series of refinement with different values for the Ni, Co and Al stoichiometry, Li-Ni mixing and Li isotropic ADP.

- To explore how deviations from the assumed Ni, Co and Al stoichiometry affect the refined structural parameters, a series of refinements were performed for $0.75 < n_{3a}^{Ni} < 0.9$, $0.1 < n_{3a}^{Co} < 0.25$, and $0 < n_{3a}^{Al} < 0.15$ (with no Li-Ni site mixing and a constant Li isotropic ADP). The refined occupancies of Li and O as a function of different Ni, Co and Al stoichiometry are shown as contour plots in Figures 4a and 4b, respectively. The refined occupancies of Li and O are highly affected by the Ni stoichiometry as evidenced by contours almost parallel to tie lines corresponding to constant Ni stoichiometry. Deviation from the nominal Ni, Co and Al stoichiometry (effectively Ni stoichiometry) by ±0.01 leads to ±0.009 variation in the Li and O occupancies (Table S3), which is comparable to the estimated standard deviation; variations in the O coordinate and the anisotropic ADPs are within in the estimated standard deviations.

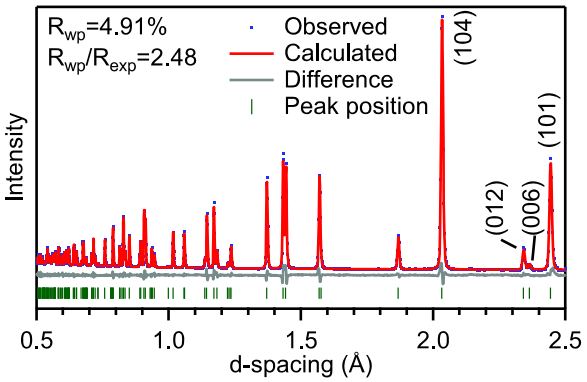

Figure 3. The best refinement profile against the NPD pattern of pristine NCA with nominal Ni, Co and Al stoichiometry and no Li-Ni mixing.

- To explore how deviations from the assumed Li-Ni mixing and Li isotropic ADP affect the refined structural parameters, a series of refinements were performed for $0.00 < n_{3a}^{Li} < 0.05$ and 0.5 Å$^2 < B_{iso}^{Li} < 1.5$ Å^2. We found that the refined Li occupancy was strongly dependent on both Li isotropic ADP and Li-Ni mixing (Figure 4c) while O occupancy was more dependent on Li-Ni mixing than Li isotropic ADP (Figure 4d). Variation of Li-Ni mixing from 0 to 0.01 leads to ±0.02 change in the Li and O occupancy (Table S3), which is larger than the estimated standard deviation. Variations in the O coordinate and anisotropic ADPs of Ni, Co, Al and O are within the estimated standard deviations. Similarly, the variation of the Li isotropic ADP from 0.9 to 1.1 Å^2 leads to ±0.02 change in the Li occupancy but only ±0.002 change in the O occupancy; variations in the O coordinate and anisotropic ADPs are within the estimated standard deviations (Table S3).

We found that the O coordinate and the anisotropic ADPs of atoms on the transition metal layer (3a site) and O atoms (on 6c site) could be accurately quantified even if the Ni, Co and Al stoichiometry, Li-Ni mixing and Li isotropic ADP were not well known. In contrast, the refined Li and O occupancies can deviate from the actual values by a few times of the estimated standard deviation even when the Li-Ni mixing or the Li isotropic ADP assumed for the structural model changes by a small value (±0.005 for Li-Ni mixing and ±0.1 Å^2 for Li isotropic ADP).

Rietveld refinement against only XRD data for pristine NCA.—*The impact of X-ray scattering factors on Rietveld refinement results.*—Unlike neutrons which are scattered by nuclei, X-rays are scattered by electrons, therefore, the scattering factor of an atom is affected by its oxidation state, that is, the electron density and density distribution. The differences in the scattering factors between free neutral and ionic atoms are most pronounced for s ($=Q/4\pi$) <0.2~0.3 Å^{-1} (Figure 5a), which includes six intense Bragg peaks, i.e. (003), (101), (006), (012), (104) and (015), for NCA (Figure 5b). Consequently, the refinement results will depend on the choice of the X-ray scattering factors of atoms in the structural model and the Q-range used for refinement. Usually, the X-ray scattering factors of free neutral or ionic (based on the atom's formal charge) atoms are adopted for the structural model. However, the free-atom scattering factor can deviate substantially from the actual scattering by an atom in the crystalline lattice. Indeed, full charge transfer between atoms rarely occurs so that the actual charge density on an atom deviates

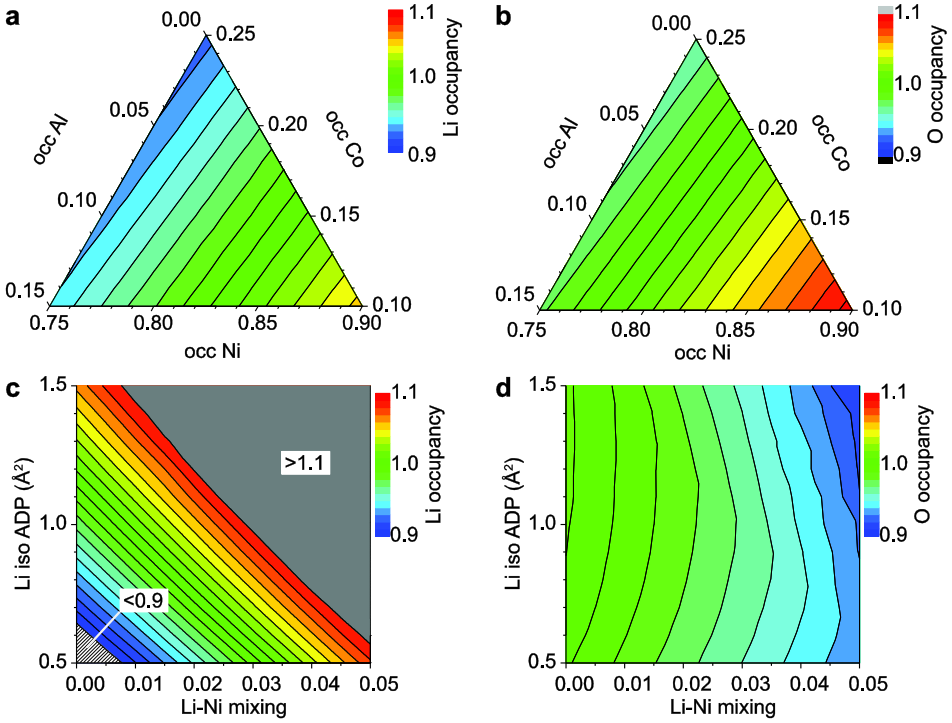

Figure 4. Ternary contour plots of the refined (a) Li and (b) O occupancies, shown in color, as a function of the Ni, Co, and Al composition; Li-Ni mixing (n_{3b}^{Ni}) and Li isotropic ADP (B_{iso}^{Li}) are assumed to be 0 and 1 Å^2, respectively. The contour lines parallel to tie lines corresponding to constant Ni occupancy indicates that Li and O occupancies are strongly correlated with the Ni occupancy. Contour plots of the refined (c) Li and (d) O occupancies, shown in color, as a function of n_{3b}^{Ni} and B_{iso}^{Li} with the nominal Co and Al stoichiometry. The Li occupancy is correlated with Li-Ni mixing and Li isotropic ADP, while the O occupancy is strongly correlated with Li-Ni mixing only (as indicated by the almost vertical contour lines).

from its formal charge.[21,22] The actual scattering factors of atoms in NCA and similar oxides have not been determined.

We performed a series of Rietveld refinements to examine how the refined structural parameters are affected by different choices of the scattering factors. In addition to neutral atoms, the oxidation states of +2, +3 for Co and Ni, +3 for Al, +1 for Li, and −1 and −2 for O were considered. For each structural model, the oxidation states of Co and Ni were constrained to be the same, and each type of atom could adopt the scattering factor of any of the oxidation states described above. This yields 36 different combinations of scattering factors for the NCA structure (descriptions of the 36 combinations are listed in Table S4). As for the NPD refinement described in the previous section, the nominal stoichiometry was assumed for Ni, Co and Al with no Li-Ni mixing, and the Li isotropic ADP was fixed to 1 Å^2, which is within the average Li ADP reported for $LiCoO_2$[19] and $LiNiO_2$[23] by NPD measurements.

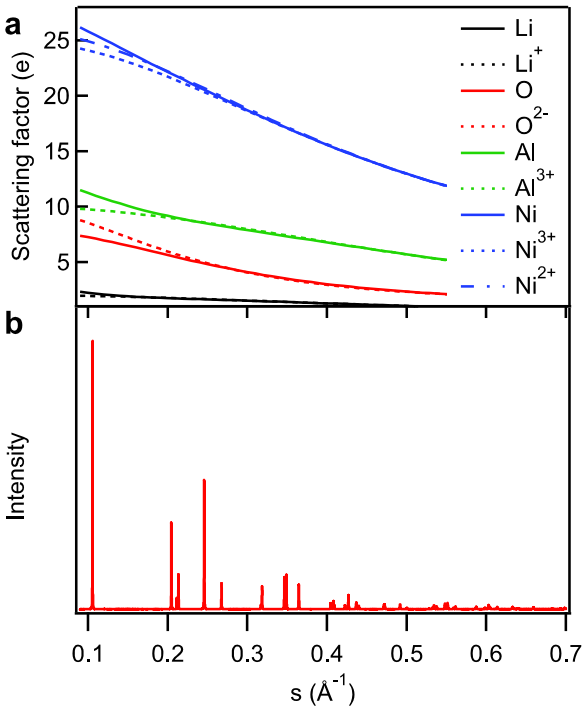

Figure 5. (a) The scattering factors of free neutral and ionic atoms.[30] (b) The XRD pattern of pristine NCA.

The different combinations of scattering factors for Rietveld refinements led to wide variations in the quality of fit measured by the R_{wp}-factor (Figure 6a). The structural model with Li, Ni, Co, Al^{3+} and O^- has the lowest $R_{wp} = 8.764\%$, which is only marginally better than the R_{wp} (8.768%) corresponding to the structural model with all neutral atoms, while the structural model with the formal charges (Li^+, Ni^{3+}, Co^{3+}, Al^{3+}, and O^{2-}) shows a substantially worse quality of fit ($R_{wp} = 8.880\%$).

The refined structural parameters also varied widely depending on the scattering factors used for the structural model (Figures 6b and 6c). For example, the O occupancy obtained for the structural model with neutral atoms and atoms of formal charges is 1.05 and 0.98, respectively, yielding 0.07 difference (Figure 6b). The variation in structural parameter, from Rietveld refinement of all 36 different oxidation state combinations, is an order of magnitude higher than the estimated standard deviation from an individual Rietveld refinement (Table S6). This demonstrates that the refined values are substantially affected by the choice of the scattering factors used for atoms in the structural model.

Although R_{wp} is often used to evaluate and compare structural models,[24] the structural model with the lowest R_{wp} in Figure 6a does not necessarily correspond to the most accurate structure of NCA. In the present case, a lower R_{wp} only indicates that the structural model provides a better fit to the electron density distribution rather than the atomic/nuclear density distribution in the actual structure. For example, because O^{2-} has a higher electron density than neutral O, the refinement of the structural model with O^{2-} leads to a higher site occupancy factor of oxygen than the structural model with neutral O (Figure 6b).

As substantial differences in the scattering factors only exist in the low-s regions, we could reduce the difference in the quality of fit (Figure 6d) and the variation in the refined structural parameters

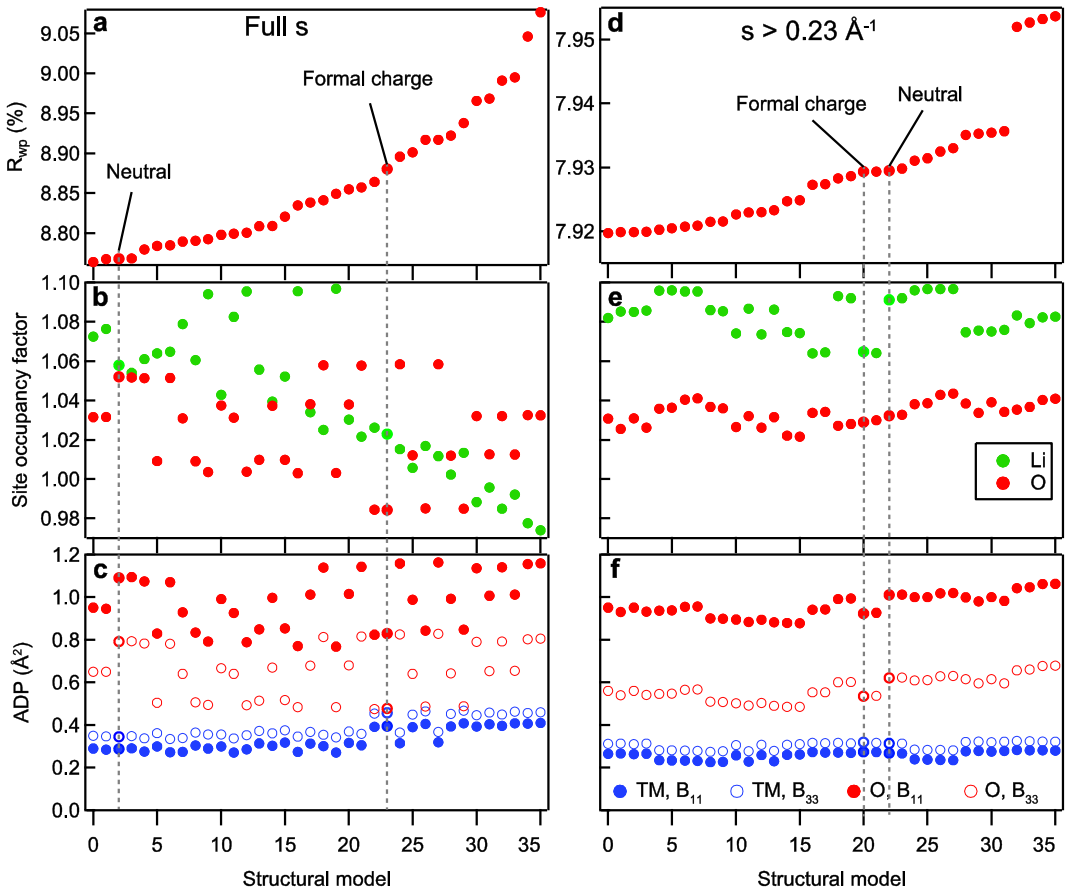

Figure 6. (a) The quality of fit measured by R_{wp} for Rietveld refinements of structural models with different combinations of scattering factors against the full s-range of the XRD pattern. Refined values of (b) the Li and O occupancies and (c) the anisotropic atomic displacement parameters (ADP) obtained from the corresponding refinement against the full range of the XRD pattern. (d) The quality of fit when the low-s region ($s < 0.23$ Å^{-1}) is excluded from the refinement. Refined values of (e) the Li and O occupancies and (f) the anisotropic ADPs obtained from Rietveld refinements when the low-s region is discarded. The scattering factors assumed for each structural model can be found in Table S5. The B_{11} and B_{33} components of the anisotropic ADPs are parallel to *a* and *c*-axis, respectively.

(Figures 6e and 6f) by excluding Bragg reflections from the low-s region ($s < 0.23$ Å^{-1}) from the refinement. The variation in values for the structural parameters obtained from 36 different models are only a factor of 2∼5 times larger than the estimated standard deviations from an individual Rietveld refinement (Table S6). Meanwhile, only the estimated standard deviation of oxygen occupancy increases by a factor of ∼2 (from 0.0016 to 0.0034), and no substantial increase in the estimated standard deviations is observed for other structural parameters. Hence, the effects of the atomic oxidation state on the Rietveld refinement result can be mitigated by excluding the low-s region; the intensities at high-s region are more sensitive to scattering of the core electrons that are not affected by the oxidation state.

Impact of Ni, Co and Al stoichiometry, Li-Ni mixing and Li isotropic ADP on Rietveld refinement result.—To evaluate parameters other than the scattering factor on the refinement results, we used scattering factors for neutral atoms in the structural model and excluded $s < 0.23$ Å^{-1} from the refinement.

- The effects of Ni, Co and Al stoichiometry variation on the Li and O occupancies were explored for $0.75 < n_{3a}^{Ni} < 0.9$, $0.1 < n_{3a}^{Co} < 0.25$, and $0 < n_{3a}^{Al} < 0.15$, with no Li-Ni mixing and constant Li isotropic ADP at 1 Å^2. The refined occupancies of Li and O are highly dependent on the Al occupancy when the total occupancy at the 3a site is fixed to 1 (Figures 7a and 7b, respectively), since the contour lines of both Li and O occupancies are almost parallel to lines corresponding to constant Al occupancy. Variation in the Ni, Co and Al stoichiometry by ±0.01 leads to ±0.005 change in the Li and O occupancies, which is comparable to the estimated standard deviation (Table S7); the corresponding changes in the anisotropic ADP of atoms on 3b site and O are well within the estimated standard deviation (Table S7).
- The effects of Li isotropic ADP and Li-Ni mixing, with nominal Co and Al composition, on Li and O occupancies are shown in Figures 7c and 7d, respectively. Variation in the Li-Ni mixing between 0 and 0.01 leads to ±0.07 and ±0.005 change in the Li and O occupancies, respectively (Table S7). In contrast, variation in the Li isotropic ADP between 0.9 and 1.1 Å^2 leads to only ±0.02 and ±0.003 change in the Li and O occupancies, respectively (Table S7).

Accuracy of Rietveld refinement against XRD data.—When the low-s region (0.23 Å^{-1}) is excluded from the refinement, the O coordinate and the anisotropic ADP of atoms on the 3a site and O can be accurately quantified. The accuracy of the O occupancy is limited to ±0.01 due to the undetermined, actual scattering factors for atoms in NCA. The Li occupancy is highly dependent on even small variations (±0.005) in Li-Ni mixing. This suggests that Li-Ni mixing can be well quantified even when there is a large error associated with the Li occupancy.

Combined neutron and X-ray refinement for pristine NCA.—*Establishing appropriate X-ray scattering factors.*—In a combined refinement, a common structural model is refined against both NPD and XRD datasets simultaneously. The two different diffraction patterns provides more structural information to allow unconstrained refinement of a greater number of structural parameters. Due to the

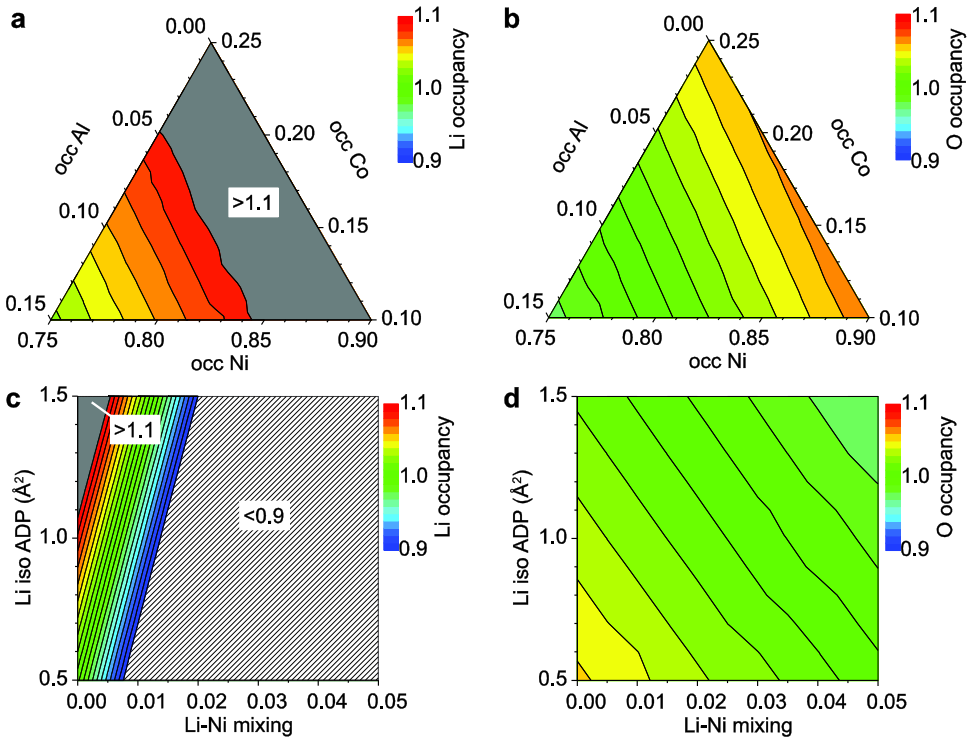

Figure 7. Ternary contour plots of the refined (a) Li and (b) O occupancies, shown in color, as a function of the Ni, Co, and Al composition. The Li-Ni mixing (n_{3b}^{Ni}) and Li isotropic ADP (B_{iso}^{Li}) are assumed to be 0 and 1 Å^2, respectively. The contour lines parallel to tie lines corresponding to constant Al occupancy indicates that Li and O occupancies are strongly correlated with the Al occupancy. The refined (c) Li and (d) O occupancies are shown in color as a function of n_{3b}^{Ni} and B_{iso}^{Li} with the nominal Co and Al stoichiometry. The Li occupancy is more correlated with Li-Ni mixing than Li isotropic ADP, while the O occupancy is correlated with both Li-Ni mixing and Li isotropic ADP.

different scattering physics of neutron and X-ray, the nuclear (i.e., atomic) occupancies are directly probed by neutron scattering, while for X-ray scattering the atomic occupancies are inferred based on the electron density defined for the atom in the structural model via selection of the X-ray scattering factor (Figure 6b). To ensure the structural model provides a good description of both the electron density distribution (as measured by XRD) and the nuclear/atomic density distribution (as measured by NPD) of the actual structure, the X-ray scattering factors of Li, Ni, Co, Al and O need to be defined appropriately to reflect the actual electron density of the atoms within the crystalline lattice.

The actual scattering factor of the atoms within the crystalline lattice were approximated by composite scattering factors—linear combinations of the scattering factors corresponding to the neutral and ionic (Ni^{3+}, Co^{3+}, and O^{2-}) states. The composite scattering factor was evaluated by refining the ratio between the scattering factors corresponding to the two different states in a combined neutron and X-ray refinement. Given the small scattering factor of Li and the small amount of Al in the actual structure, changes in the scattering factors of Li and Al make little impact on the refinement results and neutral Li and Al scattering factors were assumed in the structural model.

The refined composite X-ray scattering factors suggests that the data are best modeled as neutral atoms for Ni and Co and a linear combination of 20% neutral O and 80% O^{2-} for O. This result holds even if when different Al occupancies (0∼0.1) are assumed for the structural model. The composite scattering factors are different from the combination that yielded the smallest R_{wp} in Figure 6a. Combined refinement using the composite X-ray scattering factors with nominal Al occupancy yielded more credible values for the Li and O occupancy factors (0.995 and 0.996, respectively) than structural models with neutral atoms or atoms of formal charge (Figure 8, Table S8).

Impact of Al stoichiometry on the combined Rietveld refinement.— Reliability of the refined structural parameters was evaluated by varying the Al occupancy between 0 and 0.1. The corresponding variations in ADP, O coordinate, and Li-Ni mixing are well within their estimated standard deviations (Figure 9), so the errors of these structural parameters are determined by the quality of the data (e.g. signal-to-noise, 2θ resolution, and Q-range) and not the value of the Al occupancy. The occupancy factors of Li, O, and Co are correlated and change linearly with the Al occupancy (Figure 9): ±0.01 variation in Al occupancy introduces ±0.006, ±0.006 and ±0.002 variation in the Li, O and Co occupancy, respectively. Therefore, to obtain <0.01 accuracy in the Li, O and Co occupancy, the Al occupancy has to be determined at least with a precision of ±0.015.

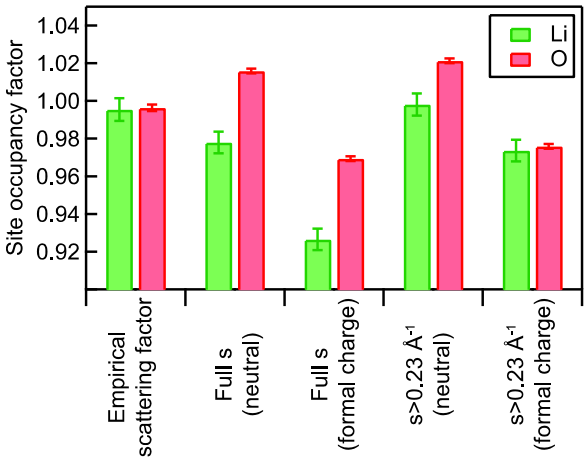

Figure 8. The site occupancy factors of Li and O obtained from combined neutron and X-ray refinement with a fixed Al occupancy at 0.05. The X-ray scattering factors and the s range of the XRD pattern used for the combined refinement are labeled explicitly.

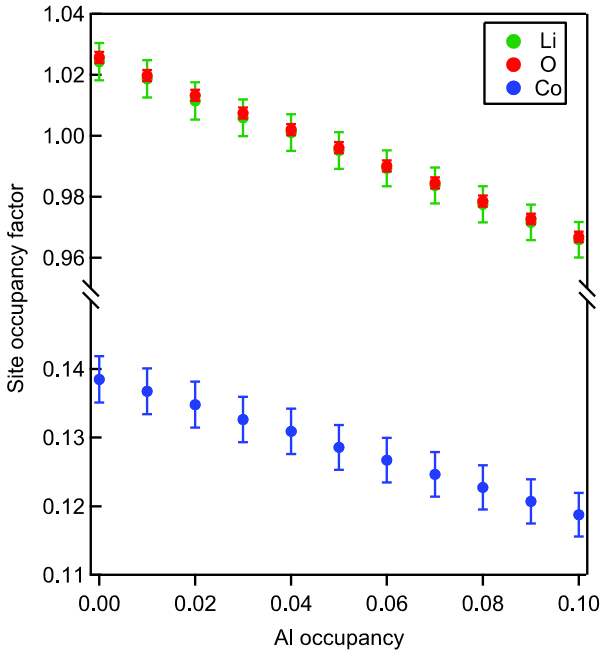

Figure 9. The site occupancy factors of Li, O, and Co obtained from combined neutron and X-ray refinement when different Al occupancy is assumed for the structural model.

Rietveld refinement for electrochemically cycled NCA samples.—Beyond analysis of the pristine electrode material, powder diffraction methods are widely used to evaluate structural changes that occur during electrochemical cycling, including under operando conditions. We examined a series of electrochemically-cycled NCA samples with NPD only, XRD only and combined NPD-XRD refinement. The electrochemical history of the samples used for the refinement is shown in Table I.

Combined neutron and X-ray Rietveld refinement has the potential to give the best structural model. However, the challenge for combined neutron and X-ray refinements is ensuring the same electrochemical state of the electrode, particularly for operando measurements conducted at separate neutron and X-ray facilities. Refinement of a common set of lattice parameters against both NPD and XRD, showed offsets in the observed and the calculated peak positions for the NPD data (Figures 10a and 10b), indicating different lattice parameters for the NPD and XRD samples. This discrepancy likely arises from sample inhomogeneity and corresponds to a difference of ~0.05 Li. To ensure refinement against the correctly measured intensity profile, lattice parameters were refined individually for each dataset while common atomic coordinates, occupancies, and ADPs were refined for both NPD and XRD datasets (Figures 10c and 10d). The occupancies of Al and Co were fixed at 0.05 and 0.13, respectively, and the composite X-ray scattering factors identified for pristine NCA structures were used (a linear combination of 80% O^{2-} and 20% neutral O for O, and neutral atoms for the rest of the atoms).

For Rietveld refinements against a single NPD or XRD pattern, in addition to constraints applied in the combined refinement, the Li isotropic ADP was fixed at 0.9 $Å^2$, the value from the combined refinement of pristine NCA (Table S8). The Li occupancy was fixed at the value corresponding to the amount of unreacted Li per formula unit of NCA. The amount of unreacted Li was determined by subtracting the amount of reacted Li that was directly measured from electrochemistry. The Li occupancy determined from the electrochemical measurement is consistently lower than that obtained from the combined refinement by at least 0.02 (Figure 11). Since the Coulombic efficiency cannot be greater than 100%, the Li occupancy estimated from electrochemistry should always be less than or equal to and provide an upper limit for the actual Li occupancy.

Table I. The electrochemical cycling history of different samples.

Sample name	Electrochemical cycling history	Current rate
c 4.3 V	Charged to 4.3 V	C/20
c 4.5 V	Charged to 4.5 V	C/20
c 4.7 V	Charged to 4.7 V	C/20
d 2.0 V	Charged to 4.7 V and then discharged to 2.0 V	C/20

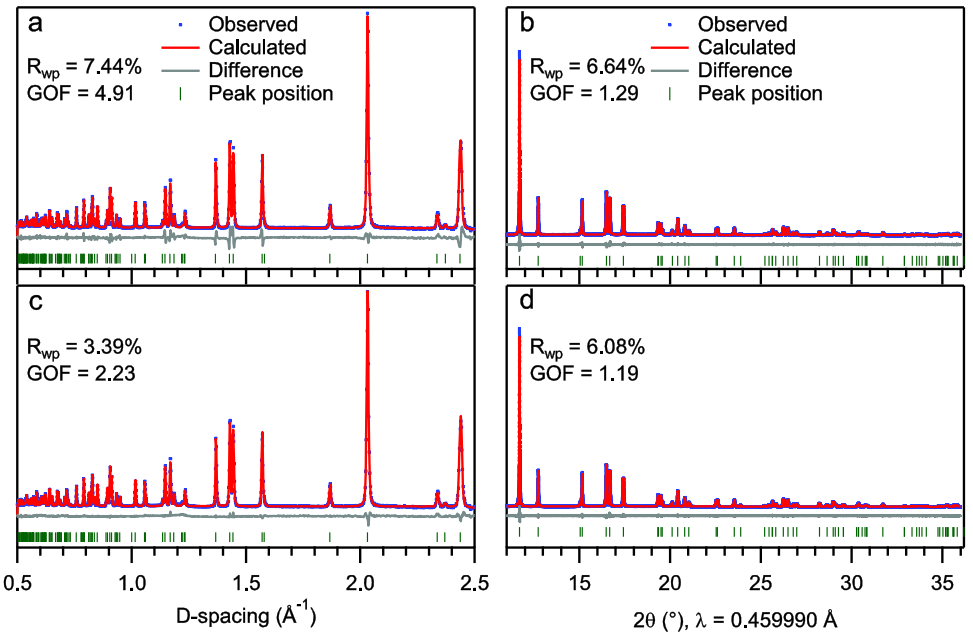

Figure 10. Rietveld refinement profiles of (a) NPD and (b) XRD data when a common set of lattice parameters is used for the combined refinement. Rietveld refinement profiles of (c) NPD and (d) XRD data when separate lattice parameters are refined against each dataset. The sample was prepared by charging to 4.7 V followed by a discharge to 2.0 V.

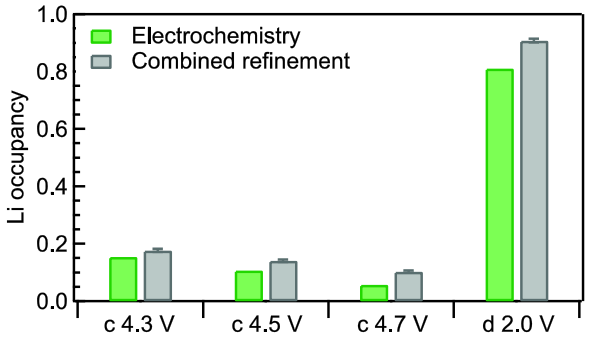

Figure 11. The Li occupancy determined from electrochemical measurement (denoted as Electrochemistry) and the combined neutron and X-ray refinement (denoted as Combined refinement).

The X-ray only refinements yield values that better match the most reliable combined X-ray-neutron refinement, than neutron only refinement. This is most evident for Li-Ni mixing and the O occupancy with the O coordinates being insensitive to the type or number of datasets used in the refinement. The Li-Ni mixing obtained from XRD refinement and combined refinement shows a value at ∼0.02, whereas the refinement against NPD patterns suggests that the Li-Ni mixing in all samples is almost 0 (Figure 12a). Because a variation of ±0.005 in the Li-Ni mixing corresponds to changes of ±0.02 and ±0.07 in the Li occupancy refined against NPD (Table S4) and XRD (Table S6) pattern, respectively, and vice versa, refinement of the Li-Ni mixing to the same accuracy will require a more accurate estimation of the Li occupancy provided for the NPD than the XRD refinement. Besides, when the Li occupancy for the structural model is less than the actual value, refinement against NPD patterns would lead to an underestimation of the refined Li-Ni due to the opposite signs of the neutron scattering length of Li and Ni, whereas refinement against XRD patterns would lead to an overestimation of the Li-Ni mixing.

The difference in the O occupancy is <0.02 between refinement against XRD patterns and the combined refinement, while refinement against NPD patterns yields consistently larger O occupancy (Figure 12b). All refinements show the same trend in the O coordinate evolution for all samples.

Rietveld refinement against only NPD or XRD patterns could discern changes in the anisotropy of ADP. The relatively large B_{33} compared to B_{11} is observed for c 4.3 V, c 4.5 V and c 4.7 V by all

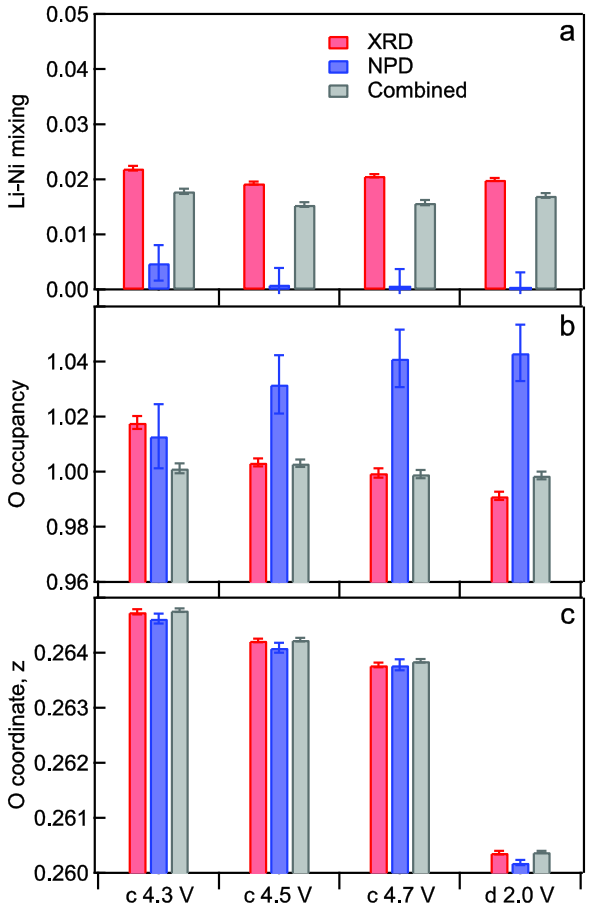

Figure 12. (a) Li-Ni mixing, (b) O occupancy and (c) O coordinate obtained from Rietveld refinement.

refinements (Figure 13). However, subtle changes in the ADPs cannot be confidently interpreted in light of the accuracy of the refinement. For example, the continuing increase in the B_{33} of Ni, Co, and Al with increasing charging voltage from 4.3 V to 4.7 V is not captured by refinement against NPD patterns. The increase in the B_{33} of O from c 4.3 V to c 4.5 V by refinement against XRD patterns (Figure 13b)

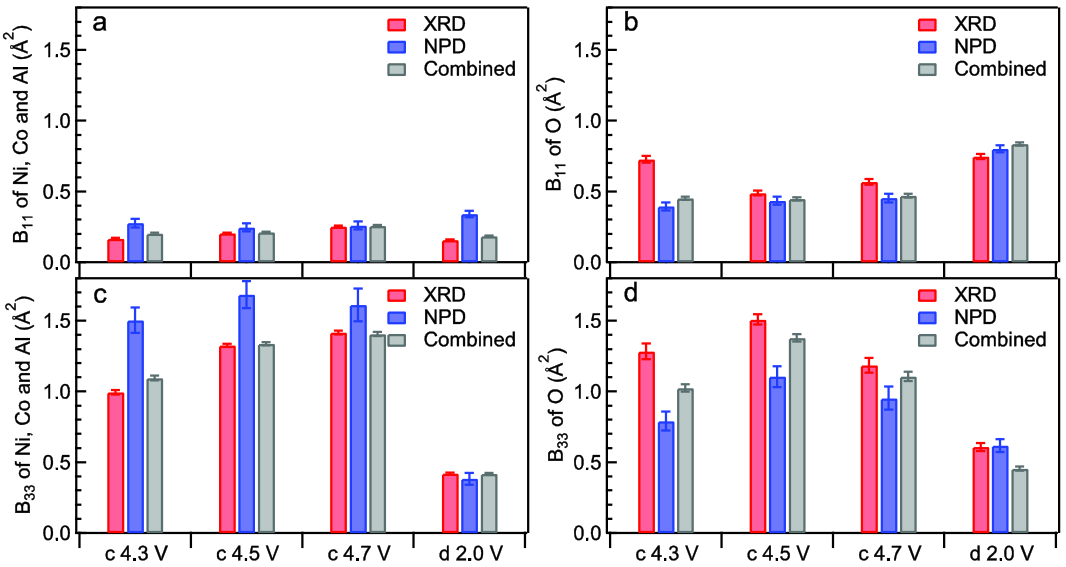

Figure 13. Anisotropic ADPs of (a, c) Ni, Co and Al and (b, d) O.

cannot be interpreted as real given the discrepancy in the B_{11} of O for c 4.3 V (Figure 13d).

Sensitivity of neutron, X-ray and combined refinement to different structural parameters.—*Effects of the X-ray scattering factor on the Rietveld refinement against XRD data.*—The X-ray scattering factors are implicit parameters of the refinement and must be properly defined and explicitly reported. Although the choices of the scattering factors do not affect the O coordinate, and hence the bond distances, the site occupancy factors can vary by several percent. This makes it difficult to interpret the composition of a given site. Because the actual scattering factors of atoms within the crystalline lattice are not readily available, an approximation can be derived from combined neutron-X-ray refinement. Our analysis suggests that for pristine NCA, the scattering factors for neutral transition metal species and a composite scattering factor for O (with the scattering factors for O and O^{2-} combined in a 1:4 ratio) are most appropriate. Further, for refinement against only XRD pattern, discarding data at low scattering angles (e.g. regions below $s = 0.23$ A^{-1} in this work) reduces the variability arising from scattering factors for different oxidation states. Although discarding part of the data leads to increased estimated standard deviation of, and higher correlation between, the refined structural parameters, this practice avoids misleading interpretation of the data.

As a corollary, the sensitivity of XRD to the oxidation state can be used to its advantage in discerning changes in the oxidation state. For example, in the Li-excess compounds, O can be oxidized (from O^{2-} to O_2^{2-} when charged to high voltages.[25] This change in the oxidation state can be detected by XRD but not NPD.

Determination of mixed metal stoichiometry.—The mixed metal stoichiometry of NCA with 4 different elements (Ni, Co, Al and Li due to site mixing) on a single crystallographic site cannot be simultaneously determined even with combined neutron and X-ray refinement. This reflects the scattering contrast between neutrons and X-rays for Al, Co and Ni: only Co exhibits large scattering contrast while the relative contrast between Ni and Al is small (the neutron scattering lengths of Ni, Co, and Al are 10.3, 2.49 and 3.45 fm, respectively; in comparison, their atomic numbers are 28, 27 and 13, respectively). In the present case, a third data set obtained from, for example, resonant XRD at Ni K-edge[26] affording contrast in the Ni scattering factor is needed to allow simultaneous refinement of the mixed metal stoichiometry. A previous structural study of $LiNi_{1/3}Mn_{1/3}Co_{1/3}O_2$ combined resonant X-ray diffraction measured near Mn K-edge, with NPD and laboratory XRD, to refine the mixed Ni, Mn and Co stoichiometry.[9]

Limits of Rietveld refinement against operando NPD/XRD dataset.—Constraints on either Li-Ni mixing or Li occupancy need to be applied for Rietveld refinement against operando NPD/XRD data sets. The electrochemistry provides a reasonably good estimate of the lower limit of the Li occupancy, and can be used to constrain this value. Accurate O coordinates and qualitative changes in the ADP can be obtained from Rietveld refinement against either NPD or XRD patterns. Accurate Li-Ni mixing can be obtained from refinement against XRD patterns by constraining the Li occupancy to a fixed value estimated from, for example, the charge/discharge capacity and elemental analysis. The accuracy of the refined O occupancy is limited to ± 0.02, hence, Rietveld refinement results alone cannot be used as the definite evidence for small changes in O occupancy.

In this work, diffraction patterns of the electrochemically-cycled samples were measured with high angular resolution and counting statistics, which are often compromised to achieve a better temporal resolution in operando measurements. The accuracy of the structural analysis depends on the reliability of the measured powdered diffraction intensities. Experimental effects that can affect the measured diffraction intensities can limit the quality of the structural analysis. This includes preferred orientation effects that can occur where the crystallite geometry is very anisotropic.[27] While spinning the sample is a common strategy to mitigate preferred orientation, this is unfeasible for operando battery experiments, where spherical particle geometries, careful electrode preparation and use of area detectors are effective strategies to ensure reliable diffraction intensities are measured. Similarly, sample absorption can impact the measured diffraction intensities leading to a systematic underestimation of the atomic displacement parameters. Intensity distortion can also arise from the incident-angle dependent absorption efficiency of the phosphors of area X-ray detectors.[28,29]

Guidelines for Rietveld structural refinement of lithium transition metal oxide electrodes.—

- Combined refinement allows simultaneous refinement of almost all structural parameters (and the X-ray scattering factors) with almost no constraints applied to the structural model, the refinement result is the least biased and provides a better structural model than refinement against either NPD or XRD pattern alone. Determination of the mixed-metal stoichiometry would require more than two types of diffraction patterns.
- O occupancy: For neutron data, the O occupancy is strongly correlated with the transition metal stoichiometry. For XRD data, the O occupancy is correlated with both mixed-metal stoichiometry and Li-Ni mixing.
- O coordinate: For NPD data, the refined O coordinate is strongly correlated with the Li isotropic ADP. For XRD data, the refined O coordinate is not correlated with any particular structural parameter.
- Li occupancy and Li-Ni mixing: Li occupancy and Li-Ni mixing are strongly correlated. Refining Li-Ni mixing with fixed Li occupancy leads to smaller uncertainty than refining Li occupancy with fixed Li-Ni mixing. For refinements against operando NPD or XRD data, it is advisable to constrain the Li occupancy according to the amount of reacted Li that can be easily obtained from the electrochemistry.

Conclusions

Rietveld refinement of the layered lithium transition metal oxide against an XRD or NPD pattern only provides limited structural information, such as O coordinate and occupancy, transition metal and oxygen ADPs. Although combining XRD and NPD data allows the determination of most of the structural parameters, the mixed metal stoichiometry (with 4 elements on a single site) cannot be determined unless a third data set (e.g. obtained from resonant scattering) is included in the refinement. For Rietveld refinement against XRD data, the use of different X-ray scattering factors for atoms of different oxidation states leads to substantial variation in the values of the refined structural parameters. However, this variation can be effectively eliminated by excluding the low-s region of XRD data from refinement. The comparison between the results obtained from XRD, NPD and combined refinement shows that the trend in the structural parameter evolution as a function of the state of charge can be captured by refinement against only XRD or NPD pattern although substantial differences exist in the absolute values. Our thorough examination of the limitations and sensitivity of the X-ray and/or neutron diffraction-based powder diffraction methods provides a practical guide to implementing and interpretation of the Rietveld analysis of the layered lithium transition metal oxides.

Acknowledgment

This research is supported as part of the NorthEast Center for Chemical Energy Storage (NECCES), an Energy Frontier Research Center funded by the U.S. Department of Energy, Office of Science, Office of Basic Energy Sciences under Award Number DE-SC0012583. This research used resources of the Advanced Photon Source, a U.S. Department of Energy (DOE) Office of Science User Facility operated for the DOE Office of Science by Argonne National Laboratory under Contract No. DE-AC02-06CH11357. A portion of this research used resources at the Spallation Neutron Source, a DOE Office of Science User Facility operated by the Oak Ridge National Laboratory. The authors thank Dr. Bao Qiu and Dr. Zhaoping Liu for preparing the pouch cells. Instrument scientists at POWGEN and

VULCAN are thanked for their help with the neutron powder diffraction measurement.

References

1. K. Mizushima, P. C. Jones, P. J. Wiseman, and J. B. Goodenough, *Mater. Res. Bull.*, **15**, 783 (1980).
2. M. M. Thackeray, W. I. F. David, P. G. Bruce, and J. B. Goodenough, *Mater. Res. Bull.*, **18**, 461 (1983).
3. M. Yoshio, H. Noguchi, J. Itoh, M. Okada, and T. Mouri, *J. Power Sources*, **90**, 176 (2000).
4. M. M. Thackeray, S. H. Kang, C. S. Johnson, J. T. Vaughey, R. Benedek, and S. A. Hackney, *J. Mater. Chem.*, **17**, 3112 (2007).
5. D. L. Zeng, J. Cabana, J. L. Breger, W. S. Yoon, and C. P. Grey, *Chem. Mater.*, **19**, 6277 (2007).
6. J. R. Dahn, U. Vonsacken, and C. A. Michal, *Solid State Ionics*, **44**, 87 (1990).
7. J. Bréger, N. Dupré, P. J. Chupas, P. L. Lee, T. Proffen, J. B. Parise, and C. P. Grey, *J. Am. Chem. Soc.*, **127**, 7529 (2005).
8. S. C. Yin, Y. H. Rho, I. Swainson, and L. F. Nazar, *Chem. Mater.*, **18**, 1901 (2006).
9. P. Whitfield, I. Davidson, L. Cranswick, I. Swainson, and P. Stephens, *Solid State Ionics*, **176**, 463 (2005).
10. A. Fossdal, H. W. Brinks, M. Fichtner, and B. C. Hauback, *J. Alloys Compd.*, **387**, 47 (2005).
11. R. E. Morris, W. T. A. Harrison, J. M. Nicol, A. P. Wilkinson, and A. K. Cheetham, *Natur*, **359**, 519 (1992).
12. C. H. Chen, J. Liu, M. E. Stoll, G. Henriksen, D. R. Vissers, and K. Amine, *J. Power Sources*, **128**, 278 (2004).
13. T. Sasaki, V. Godbole, Y. Takeuchi, Y. Ukyo, and P. Novák, *J. Electrochem. Soc.*, **158**, A1214 (2011).
14. Y. Makimura, T. Sasaki, T. Nonaka, Y. F. Nishimura, T. Uyama, C. Okuda, Y. Itou, and Y. Takeuchi, *J. Mater. Chem. A*, **4**, 8350 (2016).
15. K. An, *in* "ORNL Report". Oak Ridge National Laboratory, 2012.
16. A. Coelho, *Coelho Software*, Brisbane, Australia, 2012.
17. A. C. V. D. Larson, R.B., *in* "Los Alamos National Laboratory Report LAUR 86–784", 2004.
18. P. W. Stephens, *J. Appl. Crystallogr.*, **32**, 281 (1999).
19. H. J. Orman and P. J. Wiseman, *Acta Crystallographica Section C Crystal Structure Communications*, **40**, 12 (1984).
20. A. W. Hewat, *Acta Cryst*, **A35**, 248 (1979).
21. S. Sasaki, K. Fujino, and Y. Takeuchi, *Proceedings of the Japan Academy Series B-Physical and Biological Sciences*, **55**, 43 (1979).
22. S. Sasaki, K. Fujino, Y. Takeuchi, and R. Sadanaga, *Acta Cryst*, **A36**, 904 (1980).
23. A. Hirano, *Solid State Ionics*, **152–153**, 207 (2002).
24. B. H. Toby, *Powder Diffr.*, **21**, 67 (2012).
25. M. Sathiya, G. Rousse, K. Ramesha, C. P. Laisa, H. Vezin, M. T. Sougrati, M. L. Doublet, D. Foix, D. Gonbeau, W. Walker, A. S. Prakash, M. Ben Hassine, L. DuPont, and J. M. Tarascon, *Nature Materials*, **12**, 827 (2013).
26. J. M. Joubert, R. Cerný, M. Latroche, A. Percheron-Guégan, and K. Yvon, *J. Appl. Crystallogr.*, **31**, 327 (1998).
27. C. Nan, J. Lu, C. Chen, Q. Peng, and Y. Li, *J. Mater. Chem.*, **21**, 9994 (2011).
28. S. M. Gruner, S. L. Barna, M. E. Wall, M. W. Tate, and E. F. Eikenberry, *Proc. SPIE*, **2009**, 98 (1993).
29. G. Wu, B. L. Rodrigues, and P. Coppens, *J. Appl. Crystallogr.*, **35**, 356 (2002).
30. D. Waasmaier and A. Kirfel, *AcCrA*, **51**, 416 (1995).
31. V. F. Sears, *Neutron News*, **3**, 26 (2006).